Relation between rainfall intensity and savanna tree abundance explained by water use strategies

Xiangtao Xu[a,1], David Medvigy[a], and Ignacio Rodriguez-Iturbe[b,1]

[a]Department of Geosciences, Princeton University, Princeton, NJ 08544; and [b]Department of Civil and Environmental Engineering, Princeton University, Princeton, NJ 08544

Contributed by Ignacio Rodriguez-Iturbe, September 1, 2015 (sent for review May 18, 2015; reviewed by Manesh Sankaran)

Tree abundance in tropical savannas exhibits large and unexplained spatial variability. Here, we propose that differentiated tree and grass water use strategies can explain the observed negative relation between maximum tree abundance and rainfall intensity (defined as the characteristic rainfall depth on rainy days), and we present a biophysical tree–grass competition model to test this idea. The model is founded on a premise that has been well established in empirical studies, namely, that the relative growth rate of grasses is much higher compared with trees in wet conditions but that grasses are more susceptible to water stress and lose biomass more quickly in dry conditions. The model is coupled with a stochastic rainfall generator and then calibrated and tested using field observations from several African savanna sites. We show that the observed negative relation between maximum tree abundance and rainfall intensity can be explained only when differentiated water use strategies are accounted for. Numerical experiments reveal that this effect is more significant than the effect of root niche separation. Our results emphasize the importance of vegetation physiology in determining the responses of tree abundance to climate variations in tropical savannas and suggest that projected increases in rainfall intensity may lead to an increase in grass in this biome.

savanna | tree abundance | rainfall intensity | plant water use | competition

Despite the important role of disturbance (1–3), climatic variables, especially precipitation, are considered to be the primary determinants of the maximum achievable tree abundance in tropical savannas (4, 5). Most empirical studies consider the effects of mean annual precipitation (*MAP*) (4–6) but not precipitation variability. However, evidence is emerging that precipitation variability is also critically important for determining savanna tree abundance (7–9). In a satellite-based study that included all African savannas, maximum tree cover was found to decrease with increasing rainfall intensity after *MAP* was controlled for (7). This pattern points to a fundamental, but as yet unarticulated, mechanistic relation between rainfall intensity and tree abundance. This result also seems incompatible with classical root niche separation theory (10, 11). The theory posits that trees have deeper roots than grasses. Trees would have a relative advantage over grasses under more intense rainfall scenario because more water infiltrates into deep soil layer. Therefore, maximum tree cover should increase with increasing rainfall intensity if the classical root niche separation theory holds true.

In dry savannas (*MAP* < 1,000 mm), daily rainfall variability leads to pronounced stochasticity in the amount of soil water available to plants. The capability of efficiently using water during wet periods and while also surviving dry periods (here referred to as a water use strategy) largely defines plant competitiveness and therefore plant abundance. Here, we parameterize a biophysical tree–grass competition model with observed plant functional traits and couple the model with a stochastic rainfall generator to test whether plant water use strategies unassociated with rooting depth can explain the observed inverse correlation between rainfall intensity and tree abundance. The grasses in the model are assumed to adopt C_4 photosynthetic pathway because of the dominance of C_4 grasses in tropical savannas (12). Because we are mainly interested in the relation between maximum tree cover with rainfall intensity, the model does not incorporate disturbance events like fire, which generally reduce tree abundance (2–4). Additional information on the coupled model is given in the *Methods*.

The premise of the model is that C_4 grasses are more aggressive water users than trees (13, 14). Although the maximum stomatal conductance of C_4 grass is comparable or only slightly higher than that of trees (15, 16), the transpiration rate of C_4 grasses can be ∼five times higher than that of trees during wet periods if normalized by plant total biomass (Fig. 1*A*). This dramatic difference results from physiological and structural differences. Without the need to grow a tall and strong stem, grasses can invest more carbon into their leaves and thus have a larger leaf mass ratio (17). This differentiation, combined with large specific leaf area (18) and high water use efficiency (15, 19), allows C_4 grasses to attain a much larger relative growth rate than trees (Fig. 1*B*) when water is not limiting. The advantage of C_4 grasses decreases and finally disappears with decreasing soil moisture: trees can maintain growth in drier soils than C_4 grasses and also lose biomass more slowly when soil dries (Fig. 1*B*, *Inset*) because C_4 grasses are more susceptible to water stress (15) and have higher turnover rates (*SI Appendix*, Table S1). However, the growth advantage of C_4 grasses in wet periods is larger (Fig. 1*B*) than the advantage of trees in dry periods. Such differences can result in an advantage of grasses over trees under more intense rainfall regimes, when both extreme wet and extreme dry periods are more frequent. Trees can gain some marginal benefit through shading, but this effect is insignificant given relatively low tree abundances in tropical dry savannas (*SI Appendix*, Fig. S1).

Significance

Savannas account for 20% of global land area and support 30% of terrestrial net primary production. The biome is characterized by the coexistence of trees and grasses. Tree abundance strongly influences savanna ecosystem dynamics. Maximum tree abundance in tropical savannas is found to be negatively correlated with rainfall intensity, which remains unexplained. Through combining in situ observations, a biophysical tree–grass competition model, and a stochastic rainfall generator, we present that differentiated tree and grass water use strategies are essential to explain the phenomenon. Our findings show the importance of vegetation physiology in determining tree abundance in the biome and enhance our ability to predict future ecosystem composition and dynamics under global change.

Author contributions: X.X., D.M., and I.R.-I. designed research; X.X. performed research; X.X. analyzed data; and X.X., D.M., and I.R.-I. wrote the paper.

Reviewers included: M.S., University of Leeds.

The authors declare no conflict of interest.

[1]To whom correspondence may be addressed. Email: xiangtao@princeton.edu or irodrigu@princeton.edu.

This article contains supporting information online at www.pnas.org/lookup/suppl/doi:10.1073/pnas.1517382112/-/DCSupplemental.

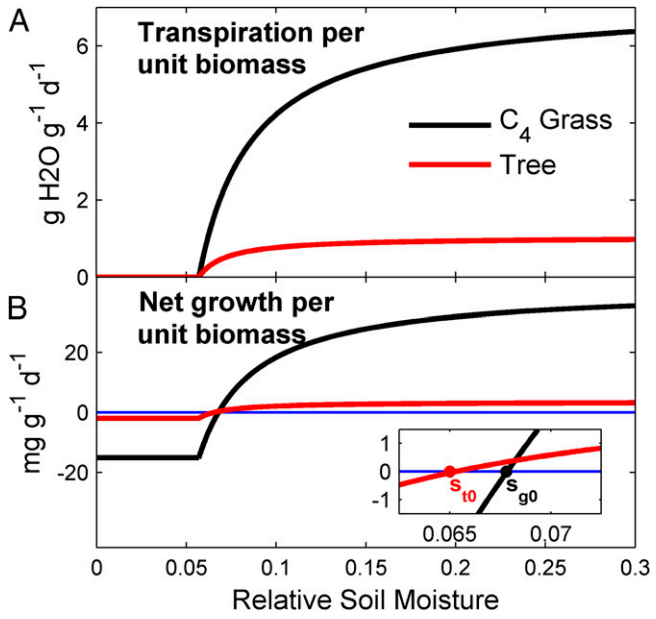

Fig. 1. Differentiated water use strategies of C_4 grass (black) and tree (red). (*A*) Transpiration. (*B*) Net growth. Net growth is defined as net primary production (NPP) minus biomass turnover. Relative soil moisture is volumetric soil moisture normalized by soil porosity. The intersections of growth curves (s_{g0} for C_4 grasses and s_{t0} for trees) with the zero-growth curve (blue) are shown in the *Inset* of *B*. The curves are generated by a saturating function of soil moisture (*SI Appendix*, Eq. **S5**) with parameters based on field and laboratory observations (*Methods* and *SI Appendix*, Table S1). Incorporation of radiative transfer and shading can induce small changes in the location of the curves (*SI Appendix*, Fig. S1).

Results and Discussion

We first test the model in a well-studied broad-leaf savanna in Nylsvley, South Africa, where trees and grasses are known to have similar rooting depth (~80 cm) (15). Using rainfall parameters derived from station observations (*SI Appendix*, Table S2), our ensemble simulations (*Methods*) generate tree–grass coexistence (Fig. 2*A*). The year-to-year oscillations in leaf area index (LAI) (calculated as leaf biomass per ground area multiplied by specific leaf area) are attributable to interannual variations in rainfall [SD, ~105 mm y^{-1}; comparable to station records (20)] from the stochastic rainfall generator. This simulated coexistence is achieved because the alternation of dry and wet days drives the alternation of tree and C_4 grass advantage, not because of disturbance or root niche separation, which was not included in the model. To better compare our simulation to field observations, we calculated the equilibrium seasonal cycles of LAI by averaging the last 50 y of the simulation (Fig. 2*B*). The ensemble-average peak wet season LAI is ~0.9 for trees and ~0.6 for grasses, close to the observed reports of 0.78 for trees and 0.5 for grasses (15). Our model overestimated dry season tree LAI in Nylsvley (reported to be ~0.1). The bias is probably attributable to the simplified phenology module in our model, in which we use a constant leaf turnover rate. Short-term turnover rate might increase in the dry season, resulting in a more complete decrease of tree LAI. Nevertheless, this bias should not influence the simulated long-term ecosystem dynamics because dry season NPP and transpiration are very small in both simulations and nature. Our results are also supported by the fact that the simulated equilibrium biomass and water fluxes are similar to reported values in Nylsvley savannas (*SI Appendix*, Table S3).

We further test the model for nine other savanna sites along the Kalahari Transect (21), Africa, where the wet season LAI of both trees and grasses have been measured (*SI Appendix*, Table S2). In our simulations, no model parameters were changed except for those determining the rainfall statistics, which were tuned to station observations. The model largely reproduces the observed LAI for both trees and grasses (Fig. 2*C*), except that it tends to underestimate grass LAI in sites where grass LAI is low (lower left black dots in Fig. 2*C*). Those sites are either very dry (~300 mm y^{-1}) or very wet (~900 mm y^{-1}). Biases at such sites are unsurprising given that our model does not include highly drought-adapted grasses in the dry sites or shade-tolerant C_3 grasses in the wet sites (22). The absence of fire in our model could be another reason. Fire can reduce the abundance of trees and thus favor grasses.

We assess whether differentiation in water use strategies is sufficient to explain the observed negative relation between rainfall intensity and maximum tree abundance by conducting simulations under a range of rainfall regimes. The relative abundance of trees and grasses is sensitive to the rainfall statistics in the coupled model (Fig. 3*A* and *SI Appendix*, Fig. S2); when rainy season length is fixed (250 d), ensemble-mean equilibrium LAI of C_4 grasses and trees is a function of both *MAP* and rainfall intensity. The abundance of trees, as indicated by equilibrium LAI, increases with *MAP*. Meanwhile, the abundance of C_4 grasses increases rapidly with rainfall in the drier half of the *MAP* range but decreases in the wetter half because the grasses are shaded out by the trees. This result is consistent with empirical studies (5, 6), but we now also directly show that coexistence is greatly modified by rainfall intensity. The abundance of C_4 grasses is much higher under an intense rainfall regime (their LAI can reach ~1.25 when intensity is ~20 mm d^{-1}) than under a mild rainfall regime (their LAI can only reach ~0.125 when intensity is ~5 mm d^{-1}). Although the effect of rainfall intensity is attained with fixed rainy season length, it still holds when the rainy season length is allowed to change (*Methods* and *SI Appendix*, Fig. S3). This pattern emerges because C_4 grasses have a relative advantage over trees when there are more wet periods (Fig. 1*B*).

To better illustrate the dependence of coexistence on rainfall intensity and to compare with empirical studies, we calculated the average equilibrium LAI of trees (an indicator of maximum tree abundance) at three intensity levels for a series of *MAP* values (Fig. 3*C*). The pattern displays a strong resemblance to observed response of tree cover to rainfall intensity (7) (Fig. 3*B*). Simulated tree abundance is most sensitive to rainfall intensity at intermediate *MAP* (500–800 mm y^{-1}). Equilibrium tree LAI in mild rainfall regimes (5–10 mm d^{-1}; Fig. 3*B*, black dots) is around twice as large as in intense rainfall regimes (15–20 mm d^{-1}; Fig. 3*B*, light gray dots). The absolute difference in LAI can reach ~0.9. The pattern still holds if we change soil parameters from sandy loam soils that are common for dystrophic savannas to clay soils that are representative of eutrophic savannas (*SI Appendix*, Fig. S4). We find that the pattern is associated with differentiated plant water use strategies between trees and grasses. The aggressive water use of grasses at high soil moisture (Fig. 1*B*) is essential. The effect of rainfall intensity weakens if the relative advantage of grasses at high soil moisture reduces (*SI Appendix*, Fig. S5). Fig. 3*D* shows an extreme scenario where the C_4 grass and tree water use strategies were swapped. As expected, the relation between tree abundance and rainfall intensity disappeared. The effect of rainfall intensity was not reversed because trees can still shade out grasses; otherwise, trees would grow better when rainfall intensity is higher (*SI Appendix*, Fig. S6). The effect of rainfall is also a function of *MAP*. When *MAP* is small, the effect of rainfall intensity is reduced because variations in rainfall intensity cannot induce significant changes during wet periods. When *MAP* is large, the dependence of tree LAI on rainfall intensity is also limited (Fig. 3 *B–D*); because soil moisture is generally high, trees can always acquire enough water, and in the extreme case, grasses are ultimately shaded out. The small effect mainly arises because total drainage increases as the rainfall regime becomes more intense (*SI Appendix*, Fig. S7).

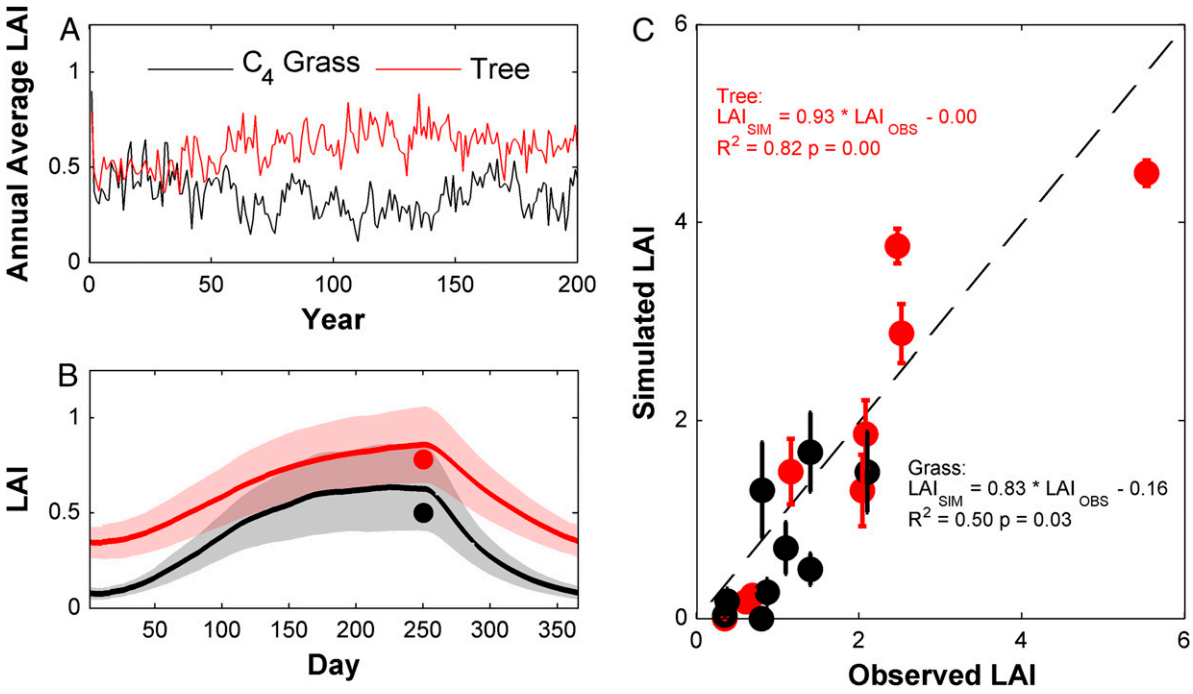

Fig. 2. Simulated tree–grass coexistence compared with field observations. (*A*) Ensemble-mean annual average LAI of C_4 grasses (black) and trees (red) from 200-y simulations using rainfall statistics in Nylsvley, South Africa. For clarity, the SD among ensemble members is not shown. (*B*) LAI seasonal cycle averaged over the last 50 y in *A* compared with observed peak wet season LAI values (solid dots). The first 250 d is the rainy season, whereas the remainder of the year is the dry season. The shading indicates SD among ensembles. (*C*) Simulated equilibrium wet season LAI of trees (red dots) and C_4 grasses (black dots) compared with observed wet season LAI across Kalahari Transect, Africa (*SI Appendix*, Table S2). Error bars represent the SD among the ensemble members.

Finally, we allow plants to adjust their rooting depth in response to biotic and abiotic environments to examine whether the plasticity of root systems (23) influences our findings. We use an evolutionary stable strategy (ESS) framework (24) to derive the rooting depth that optimizes equilibrium LAI for C_4 grasses and trees under competition (*Methods*). If there is no carbon cost

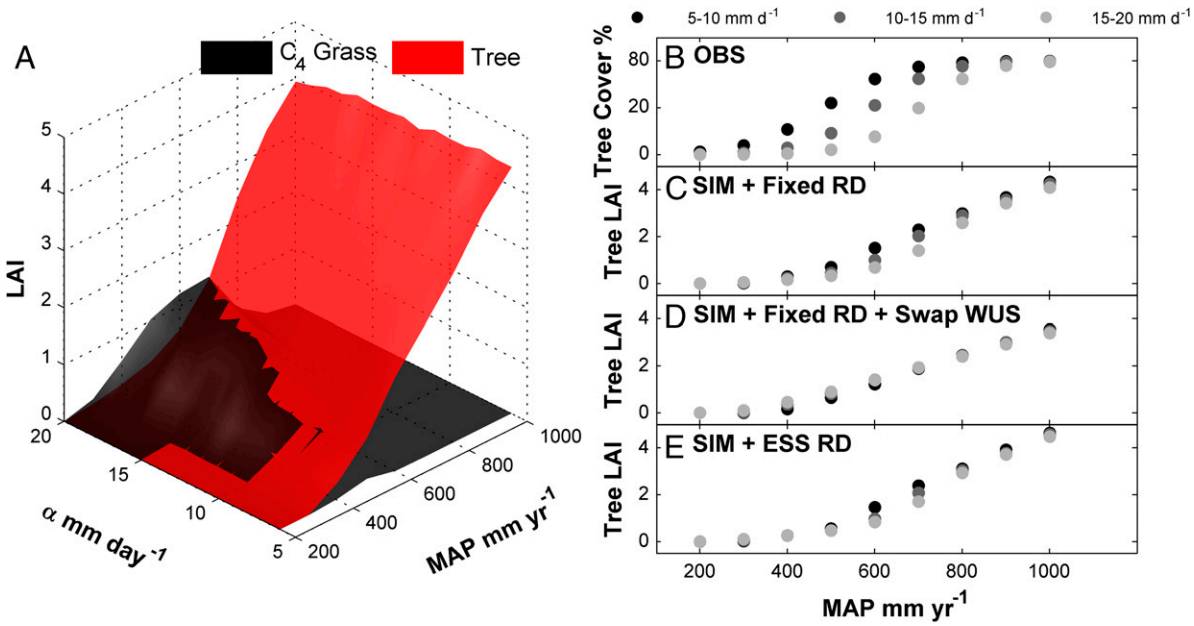

Fig. 3. Interactive effects of rainfall intensity and plant water use strategies on tree–grass coexistence. (*A*) Simulated equilibrium wet season LAI of C_4 grasses (black) and trees (red) as a function of *MAP* and rainfall intensity (α). Rainy season length is fixed as 250 d. For clarity, the SD among ensemble members is not shown. (*B*) Potential tree cover derived from remote-sensing observations at different rainfall regimes binned into three rainfall intensity levels. (*C*) Simulated tree LAI shown in *A* binned into three rainfall intensity levels. (*D*) Tree LAI from simulations in which C_4 grass and tree water use strategies (WUS) were swapped, whereas all of the other settings are the same as *C*. (*E*) Tree LAI from simulations in which rooting depth values were derived from ESS analysis without carbon cost associated with increasing rooting depth (*SI Appendix*, Fig. S8 *A* and *B*).

associated with creating and maintaining deep roots, the resulting tree and grass rooting depths are consistent with classical root niche separation theory (11), with trees having deeper roots than grasses (*SI Appendix*, Fig. S8 *A* and *B*). Root niche partitioning leads to the opposite effect compared with water use strategy differentiation because trees in this case can benefit from water infiltrating into deep soil layers under high rainfall intensity. However, this compensation is only partial, and the effect of water use strategy differentiation still dominates (Fig. 3*E*). If carbon cost is included, the ESS rooting depths of trees and grass almost converge and display a fair amount of variability because of rainfall stochasticity (*SI Appendix*, Fig. S8 *C* and *D*). Nevertheless, the simulated tree abundance is still very similar to that obtained under the assumption of fixed rooting depths (*SI Appendix*, Fig. S9).

Conclusion

In dry savannas, plants must manage the stochasticity of rainfall. Through developing more aggressive water use strategy, grasses are able to gain relative advantages over trees under high soil moisture period that is associated with high intensity rainfall. This differentiation in water use strategy creates temporal niche separation in water use between grasses and trees. With a parsimonious biophysical model, we show that this physiological differentiation is sufficient to maintain tree–grass coexistence and can explain the observed inverse correlation between maximum tree abundance and rainfall intensity in dry tropical savannas. Empirical (4–6) or modeling (1, 25) studies that use monthly or annual rainfall neglect this critical mechanism and therefore need to be interpreted cautiously. Our results imply that C_4 grasses might prosper and suppress trees in dry tropical savannas if rainfall intensity increases in the future (26). Nevertheless, careful assessment and quantification of plant water use strategies and future changes in rainfall statistics are required to accurately predict vegetation dynamics and environmental feedbacks in water-limited biomes. Finally, nutrient availability (27), CO_2 concentration (28), and disturbances like fire and herbivore (29, 30) also influence vegetation dynamics in savannas. The compounding effects of rainfall intensity, differentiated water use strategies and these factors should be addressed by future studies.

Methods

Model Description. We formulate a biophysical model based on a plant water use model (31) to capture the daily dynamics of soil moisture and tree/grass biomass in tropical savannas. In the model, trees and grasses use different water use strategies based on their observed physiological traits, and they compete for water and light, two of the most important limiting resources (32) in tropical savannas. A detailed description of the competition model and the computer code implementation can be found in Dataset S1. All of the parameters used in the model are also listed in *SI Appendix*, Table S1.

The model is then coupled with a stochastic rainfall generator. We separated each year into rainy season and dry season with rainy season length denoted as t_{rain} (day). Although rainfall in the dry season is assumed to have the same intensity (α mm d^{-1}) as in the rainy season, rainfall frequency (λ rainy day d^{-1}) in the dry season is assumed to be 20% of that in rainy season. Thus, rainfall frequency in the rainy season (λ_{rain}) can be calculated given mean annual rainfall (*MAP* mm), α and t_{rain} according to the following equation:

$$\lambda_{rain} = \frac{MAP}{\alpha \times [t_{rain} + 0.2 \times (365 - t_{rain})]}. \quad [1]$$

Rainfall is modeled as a marked Poisson process (14). The time between two rainfall events is a random variable with exponential distribution. The mean value of the exponential distribution is equal to λ_{rain} in the rainy season and $0.2 \times \lambda_{rain}$ in the dry season. Rainfall intensity is also a random variable with exponential distribution, the mean value of which equals to α. The computer codes for the model are included in Dataset S2.

Simulation Setup. For simulations of the field sites, rainfall parameters were inferred from weather station data (*SI Appendix*, Table S2). The rooting depth was set at 80 cm for both C_4 grass and trees according to field observations (15). The values and sources of other model parameters are listed in *SI Appendix*, Table S1. Only maximum surface evaporation rate was tuned to reproduce the observed evaporation–transpiration ratio in the Nylsvley site (15). For each site, we conducted 10 ensemble simulations, each for 200 y, to obtain the average tree–grass coexistence over the possible rainfall scenarios. We set the initial LAI of both trees and grasses to be 1 and the initial relative soil moisture at 0.25 for all simulations. Equilibrium wet season LAI, defined as the mean LAI within the last 50 d in wet season averaged over the last 50 y, from each simulation was calculated for both trees and C_4 grasses to compare with field observations.

We conducted simulations (Fig. 3) with 9 *MAP* values (200–1,000 mm with a step of 100 mm) and 15 α values (6–20 mm d^{-1} with a step of 1 mm d^{-1}). From Eq. **1**, there exist different combinations of λ_{rain} and t_{rain} value with a given set of *MAP* and α value. In this study, we conducted three sets of simulations where changes of α relative to baseline value (6 mm d^{-1}) were attributed differently between rainfall frequency and rainy season length: (*i*) under a given *MAP*, rainy season length was fixed and variations in α were solely balanced by changes in rainfall frequency; (*ii*) 30% of a change in α from its baseline value was attributed to changes in rainy season length, whereas the remainder was caused by a change in rainfall frequency; and (*iii*) 60% of a change in α from its baseline value was attributed to changes in rainy season length, whereas the remainder was caused by a change in rainfall frequency. We did not attribute more than 60% of variations in α to rainy season length because that would result in unrealistically low rainy season values. All of the simulations used the same model parameters and simulation setup as the simulations of the field sites. To investigate the effect of differentiated water use strategies, we also conducted simulations under different rainfall regimes in which water use strategies were swapped. In these simulations, physiological parameters were all exchanged between trees and C_4 grasses (columns 2 and 3 in *SI Appendix*, Table S1), although trees can still shade grasses. Equilibrium wet season LAI for trees was calculated as an indicator of maximum tree abundance.

The computer codes for all of the numerical simulations are included in Dataset S3.

Tree Cover Data. Potential tree cover (*PTC* in %) under a given rainfall regime was calculated using reported relations derived from moderate-resolution imaging spectroradiometer (MODIS) and tropical rainfall measuring mission (TRMM) remote-sensing data (7):

$$PTC = \frac{80}{1 + e^{-4 \times \frac{s}{80} \times (P - P_{50})}}, \quad [2]$$

$$s = 0.21 + 0.005 \times \alpha, \quad [3]$$

$$P_{50} = 308 + 21.8 \times \alpha. \quad [4]$$

In Eqs. **2**–**4**, *P* denotes mean annual precipitation (mm) and α denotes rainfall intensity (mm d^{-1}).

ESS Analysis. Under a given rainfall regime, we carried out simulations with different combinations of tree and grass rooting depths. The rooting depth of both trees and grasses were allowed to vary from 20 cm to 200 cm with a step of 20 cm (100 different combinations in total). Equilibrium (defined as the last 50 y of 200-y simulation) LAI of trees and grasses was derived for each rooting depth combination. ESS rooting depth is the combination for which neither trees nor grasses can attain significantly higher (>5%) LAI by only changing their own rooting depth. We conducted 25 ensemble simulations for each rainfall regime. Ensemble-mean ESS rooting depth and LAI were then computed. To account for the possible carbon cost associated with increasing rooting depth, we compared two ESS analyses, one with strong cost and one with no cost. In the analysis with strong cost, root mass ratio (rmr_{cost}) increases with rooting depth (*RD*):

$$rmr_{cost} = [1 + (RD - RD_0) \times I_{margin}] \times rmr. \quad [5]$$

In Eq. **5**, RD_0 is the rooting depth at which rmr_{cost} is equal to *rmr* given in *SI Appendix*, Table S2. I_{margin} denotes the marginal relative increase of rmr_{cost} associated with increase of rooting depth. RD_0 is set to 80 cm and I_{margin} is set to 5% per 20 cm for both trees and grasses based on the observed ranges of root mass ratio in nature (18). *lmr* is modified accordingly to balance the changes of rmr_{cost}. In the analysis with no cost, the tree and grass *rmr* values were set to those given in *SI Appendix*, Table S2 and do not change with rooting depth. The computer codes for ESS analysis are included in Dataset S3.

ACKNOWLEDGMENTS. This work was supported by the Princeton Environmental Institute and the Andlinger Center for Energy and the Environment at Princeton University.

1. Bond WJ, Woodward FI, Midgley GF (2005) The global distribution of ecosystems in a world without fire. *New Phytol* 165(2):525–537.
2. Staver AC, Archibald S, Levin SA (2011) The global extent and determinants of savanna and forest as alternative biome states. *Science* 334(6053):230–232.
3. Van Langevelde F, et al. (2003) Effects of fire and herbivory on the stability of savanna ecosystems. *Ecology* 84(2):337–350.
4. Lehmann CER, et al. (2014) Savanna vegetation-fire-climate relationships differ among continents. *Science* 343(6170):548–552.
5. Sankaran M, et al. (2005) Determinants of woody cover in African savannas. *Nature* 438(7069):846–849.
6. Hirota M, Holmgren M, Van Nes EH, Scheffer M (2011) Global resilience of tropical forest and savanna to critical transitions. *Science* 334(6053):232–235.
7. Good SP, Caylor KK (2011) Climatological determinants of woody cover in Africa. *Proc Natl Acad Sci USA* 108(12):4902–4907.
8. Holmgren M, Hirota M, van Nes EH, Scheffer M (2013) Effects of interannual climate variability on tropical tree cover. *Nat Clim Chang* 3(8):755–758.
9. Murphy BP, Bowman DMJS (2012) What controls the distribution of tropical forest and savanna? *Ecol Lett* 15(7):748–758.
10. Kulmatiski A, Beard KH (2013) Woody plant encroachment facilitated by increased precipitation intensity. *Nat Clim Chang* 3(9):833–837.
11. Walter H (1971) *Ecology of Tropical and Subtropical Vegetation* (Van Nostrand Reinhold Co., New York).
12. Edwards EJ, et al.; C4 Grasses Consortium (2010) The origins of C4 grasslands: Integrating evolutionary and ecosystem science. *Science* 328(5978):587–591.
13. Bond WJ (2008) What limits trees in c4 grasslands and savannas? *Annu Rev Ecol Evol Syst* 39:641–659.
14. Rodriguez-Iturbe I, Porporato A (2004) *Ecohydrology of Water-Controlled Ecosystems: Soil Moisture and Plant Dynamics* (Cambridge Univ Press, New York).
15. Scholes RJ, Walker BH (1993) *An African Savanna: Synthesis of the Nylsvley Study* (Cambridge University Press, New York).
16. Simioni G, Le Roux X, Gignoux J, Walcroft A (2004) Leaf gas exchange characteristics and water- and nitrogen-use efficiencies of dominant grass and tree species in a West African savanna. *Plant Ecol* 173(2):233–246.
17. Poorter H, et al. (2012) Biomass allocation to leaves, stems and roots: Meta-analyses of interspecific variation and environmental control. *New Phytol* 193(1):30–50.
18. Poorter H, Niinemets U, Poorter L, Wright IJ, Villar R (2009) Causes and consequences of variation in leaf mass per area (LMA): A meta-analysis. *New Phytol* 182(3):565–588.
19. Pearcy RW, Ehleringer J (1984) Comparative ecophysiology of C3 and C4 plants. *Plant Cell Environ* 7(1):1–13.
20. Fernandez-Illescas CP, Rodriguez-Iturbe I (2003) Hydrologically driven hierarchical competition–colonization models: The impact of interannual climate fluctuations. *Ecol Monogr* 73(2):207–222.
21. Koch G, Vitousek P, Steffen W, Walker B (1995) Terrestrial transects for global change research. *Vegetatio* 121(1-2):53–65.
22. Ehleringer J (2005) The influence of atmospheric CO2, temperature, and water on the abundance of c3/c4 taxa. *A History of Atmospheric CO2 and Its Effects on Plants, Animals, and Ecosystems*, Ecological Studies, eds Baldwin IT, et al (Springer, New York) Vol 177, pp 214–231.
23. Hodge A (2004) The plastic plant: Root responses to heterogeneous supplies of nutrients. *New Phytol* 162(1):9–24.
24. Smith JM, Price GR (1973) The logic of animal conflict. *Nature* 246(5427):15–18.
25. Scheiter S, Higgins SI (2009) Impacts of climate change on the vegetation of Africa: An adaptive dynamic vegetation modelling approach. *Glob Change Biol* 15(9):2224–2246.
26. Easterling DR, et al. (2000) Climate extremes: Observations, modeling, and impacts. *Science* 289(5487):2068–2074.
27. Huntley BJ, Walker BH (1982) *Ecology of Tropical Savannas* (Springer, Berlin; New York).
28. Morgan JA, et al. (2011) C4 grasses prosper as carbon dioxide eliminates desiccation in warmed semi-arid grassland. *Nature* 476(7359):202–205.
29. Liedloff AC, Cook GD (2007) Modelling the effects of rainfall variability and fire on tree populations in an Australian tropical savanna with the Flames simulation model. *Ecol Modell* 201(3–4):269–282.
30. Scheiter S, Higgins SI, Beringer J, Hutley LB (2015) Climate change and long-term fire management impacts on Australian savannas. *New Phytol* 205(3):1211–1226.
31. Zea-Cabrera E, Iwasa Y, Levin S, Rodríguez-Iturbe I (2006) Tragedy of the commons in plant water use. *Water Resour Res* 42(6):W06D02.
32. Scheiter S, Higgins SI (2007) Partitioning of root and shoot competition and the stability of savannas. *Am Nat* 170(4):587–601.